INFLUENCE OF SILVER NANOPARTICLES ON MECHANICAL AND ANTIMICROBIAL PROPERTIES OF SELECTED REINFORCED PC AND HDPE COMPOSITES

Kayode Adebesin [1], Anna M. Kłeczek [1], Mateusz Galeja [2], Jadwiga Gabor [1], Jarosław Markowski [3], Andrzej S. Swinarew [1,4*]

[1] Faculty of Science and Technology, University of Silesia, 75 Pułku Piechoty 1A, 41-500 Chorzów, Poland
[2] Spyra Prime Sp. z o.o., Przelotowa 33, 43-190 Mikołów, Poland
[3] Department of Laryngology, Faculty of Medical Sciences in Katowice, Medical University of Silesia, Francuska 20-24, 40-027 Katowice, Poland
[4] Institute of Sport Science, The Jerzy Kukuczka Academy of Physical Education, Mikołowska 72A, 40-065 Katowice, Poland
* e-mail: andrzej.swinarew@us.edu.pl

Abstract

This study investigated the influence of silver nanoparticles (AgNPs) on the mechanical and antibacterial properties of polycarbonate (PC) and high-density polyethylene (HDPE) composites reinforced with glass (GF), basalt (BF), carbon (CF), and cellulose (CEL) fibres. The mechanical properties of the composites were rigorously assessed by quantifying parameters such as impact strength, tensile strength, and elongation at break. This evaluation was performed in strict adherence to ASTM standards, ensuring reliability and consistency of the obtained data. The results demonstrated that fibre reinforcements enhanced the tensile strength of the composites, but resulted in reductions in both impact strength and elongation at break, particularly in composites containing cellulose. The addition of AgNPs further decreased impact strength and elongation at break, while slightly reducing tensile strength. The antimicrobial properties were evaluated using bacterial strains Escherichia coli (E. coli) and Staphylococcus aureus (S. aureus). Composites reinforced with glass fibre and AgNPs exhibited the highest antimicrobial efficacy compared to those containing AgNPs combined with cellulose, carbon, or basalt fibres. These findings suggest that while AgNPs enhance the antimicrobial properties, they may compromise the mechanical integrity of fibre-reinforced composites. The study contributes to the development of advanced composites with multifunctional properties for medical, sports, aerospace, construction, and engineering applications.

Keywords: *silver nanoparticles, reinforced composites, polycarbonate, high-density polyethylene, antimicrobial effects, natural fibre reinforcements.*

[Engineering of Biomaterials 173 (2025) 08]

doi:10.34821/eng.biomat.173.2025.08

Submitted: 2025-06-25, Accepted: 2025-08-01, Published: 2025-08-06

Introduction

The study of composite materials has gained considerable attention in recent years due to their ability to meet the growing demand for advanced materials with enhanced mechanical properties and reduced weight. These attributes are particularly valued in the aerospace, medicine, sports, automotive, and construction industries. Polycarbonate (PC) and high-density polyethylene (HDPE) are widely recognised for their excellent mechanical properties, durability, high chemical resistance, and versatility. However, the limitations of these polymers, such as restricted thermal stability and susceptibility to environmental degradation, necessitate the introduction of reinforcing agents to improve their performance. This research comparatively analyses composites reinforced with basalt, carbon, glass, and cellulose fibres to address these challenges.

Silver nanoparticles (AgNPs) are increasingly utilised in the development of hybrid nanostructures and composite materials [1], resulting in polymer nanocomposites. Nanocomposites consist of nanoparticles distributed throughout a matrix, often a polymer [2], leading to a product that combines the properties of both constituents [3]. The incorporation of silver nanoparticles has emerged as a viable method to enhance the mechanical, thermal, and antibacterial properties of polymer composites [4-5]. AgNPs may achieve an exceptionally tight particle size distribution and form, yet they are highly unstable due to their propensity to coagulate. Extensive studies show that AgNPs exhibit limited reactivity with most polymers. They are notable for their high surface area-to-volume ratio and potent antibacterial properties, making them valuable in areas such as food packaging and biomedical devices [6-8]. In addition to their organometallic catalytic activity, the unique features of AgNPs, derived from their nanoscale structure, enable a diverse range of applications.

Reinforcing PC and HDPE with various fibre types – namely basalt, carbon, glass, and cellulose – offers significant benefits. Basalt fibres (BF), derived from volcanic rocks, are known for their high tensile strength, thermal stability, and corrosion resistance, making them well-suited for demanding applications. Their remarkable tensile properties and exceptional stiffness-to-weight ratios have led to their adoption in high-performance industries [9-11]. Glass fibres (GF), the most commonly used reinforcement in polymer composites, provide excellent mechanical properties at a relatively low cost [12-14]. Cellulose fibres (CEL) are biodegradable, plentiful, and provide mechanical support [15-17]. Carbon fibre-reinforced polymer composites show great potential as replacements for steel and aluminium due to their strength, high specific stiffness, and lightweight influence by carbon fibre (CF) [18-20]. This makes CF useful in many industries, including construction, aerospace, pressure vessels, and medical items.

This comparative investigation assesses mechanical and antibacterial characteristics of PC and HDPE composites' reinforced with different fibre types and silver nanoparticles. By examining the behaviour of these materials under varied conditions, the study aims to identify optimal combinations of matrix and reinforcements at low concentrations. The findings are expected to contribute to the development of high-performance materials for diverse applications, addressing the limitations of conventional polymers.

Materials and Methods

HDPE pellets with a density of 0.958 g/cm³ and melt flow index (MFI) of 1.2 g/10 min at a temperature of 190°C and a weight of 5 kg were supplied by Orlen Unipetrol RPA.

Makrolon® 2600 PC pellets were purchased from Covestro, Leverkusen, Germany. They are characterised by the MFI of 13 g/10 min at a weight of 1.2 kg, 300°C, and moderate viscosity.

The reinforcements used included: basalt fibres (BCS KV02M) with a length of 13 mm, a width of 3.2 mm, and a thickness of 3.175 mm, sourced from Tech Solutions, Poland; carbon fibres with a length of 6 mm and a diameter of 3 mm, purchased from TC3 Limited, Poland; glass fibres (EC7 34 X 2) provided in the form of a string by Pabiantex Wojtas Tomaszewski Sp. J., Poland; and cellulose flakes supplied by Eko Fibre, Poland.

The compatibiliser was commercial polyether-polyol (Rokopol® D2002 CAS 25322-69-4 from PCC, Rokita SA, Brzeg Dolny, Poland). It has a density of 1.04 g/cm³ and an average molecular weight of 2000 g/mol. This compound is a linear polyoxypropylene diol with a hydroxyl number ranging from 53 to 59 mg KOH/g. Silver nanoparticles measuring 50-70 nm were obtained from Avantor Performance Materials Poland S.A. (Gliwice, Poland).

The first stage of the study involved drying all materials used for producing the composites in a DZ-3DB II vacuum drying oven at 55°C and a pressure of 760 mmHg for 6 hours. Then, 9 g of each fibre reinforcement, except AgNPs, were subjected to size reduction in a sample chamber operating at a rotational speed of 350 rpm, with 47 repetitions and a timer set for 15 minutes per repetition, continuing for 24 hours. Following this, 750 g of dried matrix material was mixed with 7.5 g of fibres and 2 mL of Rokopol® to produce composites (first group). This procedure was repeated with the addition of 0.5 g of AgNPs (second group). As a result, composites with 1% fibre filling and 1% fibre filling with 0.06% AgNPs content were obtained, respectively.

The prepared composite materials were put into a Lenze GST05 mini double-screw extruder to create molten filaments. The two-zone single-screw extruder was set to 220°C for HDPE composites and 230°C for PC composites. The extruded molten filaments were flattened into sheets and placed under an iron preform subjected to 200 bar pressure using a Ponar Wadowice UCJ3-GZ press to create test sample templates for mechanical and antimicrobial analysis. Tensile tests, Charpy impact tests, and antimicrobial tests were conducted in accordance with ASTM D638-14, ASTM D6110-18, and ISO 22196:2007(E), respectively.

TABLE 1 provides a detailed description of the produced polymer composites, specifying the composition of each formulation. Two matrix materials, PC and HDPE, were utilised, each combined with various reinforcement configurations. The reinforcements included basalt, glass, cellulose, and carbon fibres. Silver nanoparticles were incorporated into selected composites to enhance their material properties. Each composite formulation is indexed for clarity, showing the base matrix material combined with one or more reinforcements.

TABLE 1. Detailed composition of the produced composites

Matrix	Reinforcements	Index
PC	–	PC
	7.5 g BF	PC/BF
	7.5 g BF + 0.5 g AgNPs	PC/BF/AgNPs
	7.5 g GF	PC/GF
	7.5 g GF + 0.5 g AgNPs	PC/GF/AgNPs
	7.5 g CEL	PC/CEL
	7.5 g CEL + 0.5 g AgNPs	PC/CEL/AgNPs
	7.5 g CF	PC/CF
	7.5 g CF + 0.5 g AgNPs	PC/CF/AgNPS
HDPE	–	HDPE
	7.5 g BF	HDPE/BF
	7.5 g BF + 0.5 g AgNPs	HDPE/BF/AgNPs
	7.5 g GF	HDPE/GF
	7.5 g GF + 0.5 g AgNPs	HDPE/GF/AgNPs
	7.5 g CEL	HDPE/CEL
	7.5 g CEL + 0.5 g AgNPs	HDPE/CEL/AgNPs
	7.5 g CF	HDPE/CF
	7.5 g CF + 0.5 g AgNPs	HDPE/CF/AgNPs

An Olympus LEXT OLS4000 LCSM was employed to examine the surface topography of the polymer composites. This system features a dual confocal system that enhances the optical resolution of micrographs. It allows the LEXT OLS4000 to capture clear images of specimens with varying reflectivity levels by scanning a laser beam spot of less than 1 µm in diameter across each point of the examined area. A spatial pinhole is used to block out-of-focus light during image formation. Surface images were analysed with MountainsMap® Premium software (version 8.2.9468).

The JEOL (model JSM-6300F) scanning electron microscope was used to observe the reinforcements' pore size distribution and surface morphology. It was equipped with a field emission gun and an accelerating voltage of 10 keV. Platinum was sputtered onto each sample in an even layer for three minutes. The secondary electron imaging (SEI) mode was used to capture SEM images, with a working distance of 10 mm and a magnification of 10,000x.

For impact strength testing, a pendulum-type Impact Tester (Werkstoffprüf Maschinen, Leipzig, Germany) was utilised. The tester, with a 937 g weight and a 4 J pendulum, was employed to analyse samples according to ASTM D6110-18 standard. Five specimen samples of each type were tested, each measuring 55 mm x 10 mm x 10 mm and containing a 2.0 mm deep V-shaped notch. The impact speed was 2.92 m/s, and the distance from the sample notch to the pivot point measured 220 mm. A hammer with an impact energy of 4 J was applied at room temperature, and a breakthrough was observed in all five samples after impact.

The strength properties were determined by means of a static tensile test of dog-bone specimens (165 mm x 12.5 mm x 3 mm). They were measured using a Shimadzu AG-Xplus tensile testing machine, coupled with a Shimadzu SIE-560SA extensometer and analysed using Windows®-based TRAPEZIUM X-V software. The tests were conducted at room temperature, with a cross-head speed of 1 mm/min and a sampling frequency of 22 Hz (46 msec), according to ASTM D638-14. Five specimens were tested for each composite until the final failure.

The composites' antibacterial activity was assessed according to the ISO 22196:2007 (E) standard titled "Plastics – Measurement of antibacterial activity on plastic surfaces. "The reference strains used were Escherichia coli DSM 1576 (E. coli) and Staphylococcus aureus DSM 346 (S. aureus). The exposed outer surfaces of the test specimens were analysed. Each specimen was placed in a sterile Petri dish with the test surface facing upward. A 0.4 mL aliquot of the bacterial suspension (concentration of the bacterial inoculum 6 × 10^5 bacteria/mL) was pipetted onto the surface and covered with a sterile polyethylene film, which was gently pressed to ensure uniform contact and prevent leakage beyond the edges. The dishes were sealed and incubated for 24 hours at 35°C and 90% relative humidity to maintain appropriate microbial growth conditions. After incubation, the bacteria were recovered from the surfaces, and the resulting suspensions were serially diluted tenfold to obtain countable concentrations. The diluted samples were plated on nutrient agar and incubated for colony development. Neutralisation procedures were performed in accordance with PN ISO 18593:2005 and PN ISO 14562:2006. Colony-forming units (CFU) were counted, and the number of viable bacteria per cm² on each sample was calculated. The reference sample for antibacterial testing was coated with AgNPs. Each test was repeated three times under identical environmental conditions to ensure reproducibility and measurement consistency.

The mean antibacterial activity (R) of each composite sample was calculated using the following mathematical equation:

$$R = (Ut - U0) - (At - U0)$$
$$R = Ut - At.$$

where: U0 – the mean decimal logarithm of the count of viable bacteria (cells/cm²), obtained from untreated samples after inoculation; Ut – the mean decimal logarithm of the count of viable bacteria (cells/cm²), obtained from untreated samples after 24 h; At – the mean decimal logarithm of the count of viable bacteria (cells/cm²), obtained from treated samples after 24 h.

Results and Discussions

FIGs 1-4 illustrate the surface topography analysis of the reinforcements employed in the production of the composites, before and after size reduction. The surface morphological features directly influence their mechanical performance. The topography of the materials (GF, CF, BF, and CEL) transitioned from rough and irregular surfaces to smoother surfaces with varying degrees of porosity.

FIG. 5 shows the surface microstructure of BF, CF, GF, and AgNPs. As seen in FIG. 5, AgNPs displayed a smooth surface morphology, while BF and GF showed clustered crystalline structures, and CF exhibited a fibrous crystalline structure. These differences could be attributed to the varying rates of hygroscopy when exposed to moisture in the atmosphere during analysis. SEM micrographs could not be obtained for cellulose because SEM's focused beam of high-energy electrons could not generate signals due to poor charge mobility on the surface of cellulose fibres.

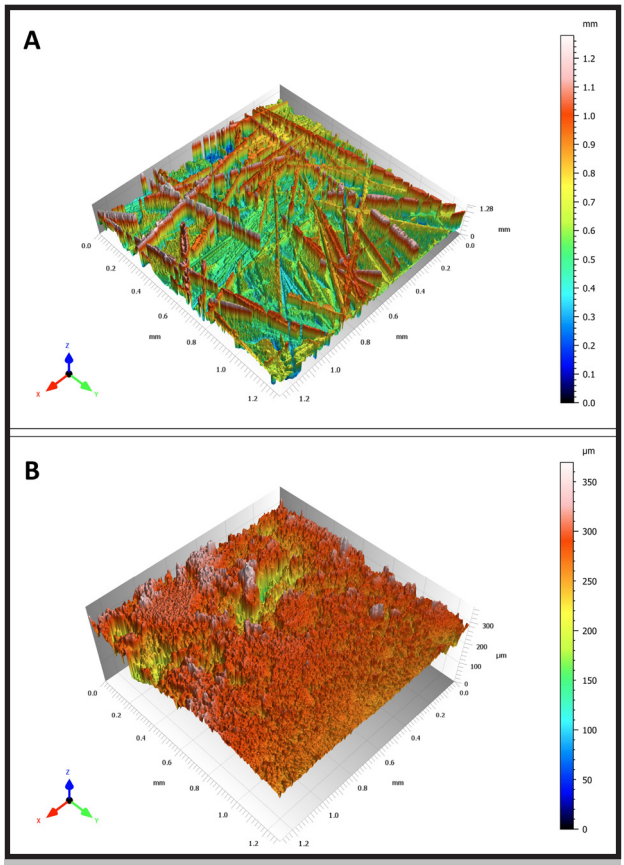

FIG. 1. Surface topography of short glass fibre: (A) before size reduction, (B) after size reduction

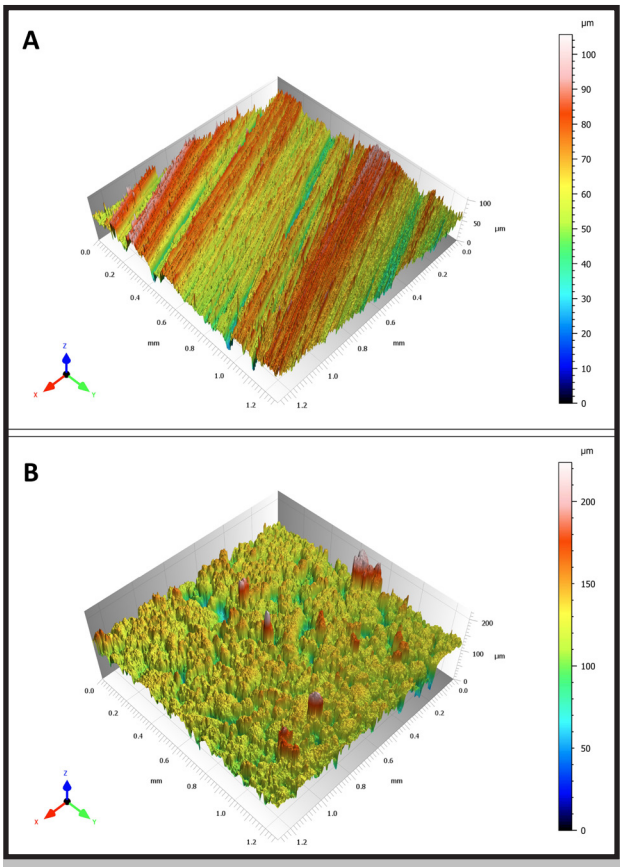

FIG. 2. Surface topography of short carbon fibre: (A) before size reduction, (B) after size reduction

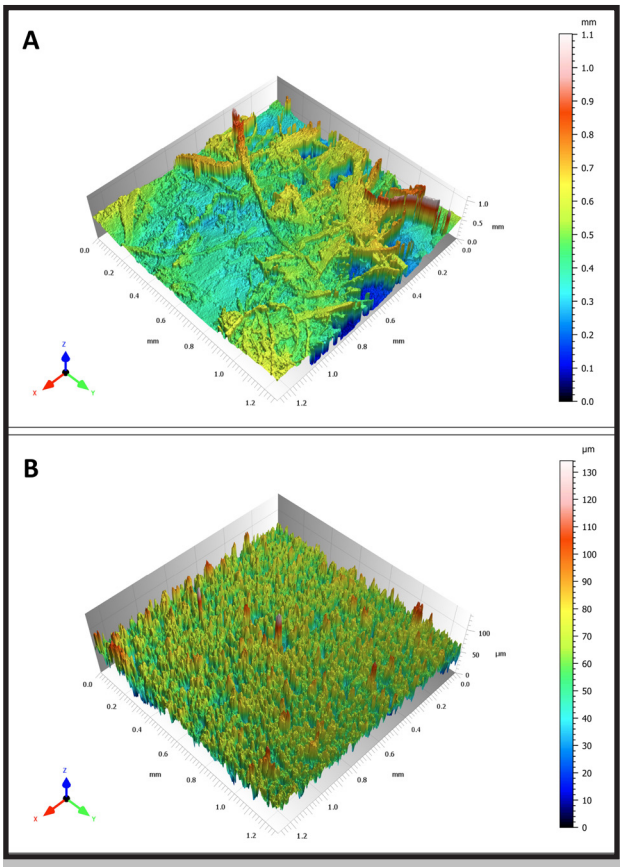

FIG. 4. Surface topography of cellulose: (A) before size reduction (B) after size reduction

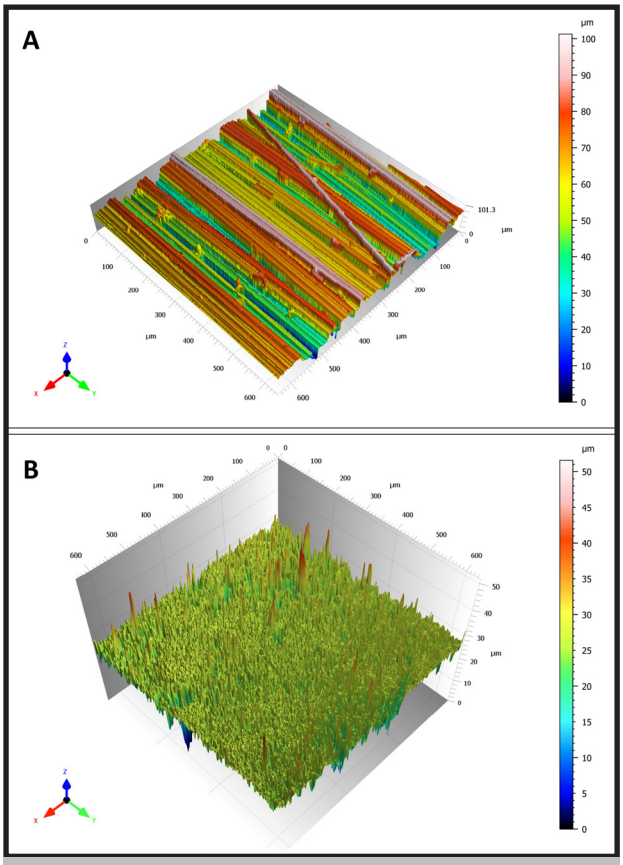

FIG. 3. Surface topography of basalt fibre: (A) before size reduction (B) after size reduction

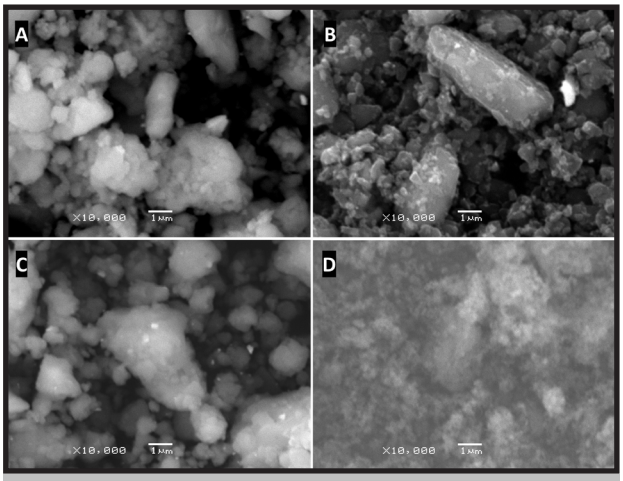

FIG. 5. Scanning electron microscopy images of: (A) reduced basalt fibre, (B) reduced carbon fibre, (C) reduced glass fibre, (D) silver nanoparticles

The results presented in TABLES 2 and 3 provide insights into the mechanical properties of HDPE and PC composites with various reinforcements. Each composite sample was evaluated based on three key mechanical properties: impact strength, tensile strength, and elongation at break. These values demonstrate how different reinforcements influence the mechanical performance of the PC and HDPE matrices, informing potential applications based on strength, flexibility, and durability requirements.

TABLE 2. Mechanical properties of HDPE-based composites

Sample	Impact strength (kJ/m²)	Tensile strength (MPa)	Elongation at break (%)
HDPE	7.18 ± 0.12	24.02 ± 0.31	375.31 ± 42
HDPE/GF	6.16 ± 0.08	26.61 ± 0.42	326.24 ± 58
HDPE/CF	6.65 ± 0.08	27.99 ± 0.22	290.81 ± 28
HDPE/BF	6.27 ± 0.09	27.11 ± 0.34	301.47 ± 34
HDPE/CEL	6.11 ± 0.12	25.32 ± 0.39	285.32 ± 67
HDPE/GF/AgNPs	5.56 ± 0.14	25.76 ± 0.45	299.49 ± 21
HDPE/CF/AgNPs	5.69 ± 0.12	26.86 ± 0.60	265.66 ± 31
HDPE/BF/AgNPs	5.60 ± 0.06	26.33 ± 0.32	284.57 ± 43
HDPE/CEL/AgNPs	5.45 ± 0.09	24.99 ± 0.06	262.51 ± 19

TABLE 3. Mechanical properties of PC-based composites

Sample	Impact strength (kJ/m²)	Tensile strength (MPa)	Elongation at break (%)
PC	6.71 ± 0.18	49.76 ± 4.32	28.51 ± 0.82
PC/GF	6.42 ± 0.10	59.71 ± 9.46	25.34 ± 0.2
PC/CF	6.53 ± 0.08	63.42 ± 1.44	21.31 ± 0.32
PC/BF	6.49 ± 0.13	62.05 ± 1.51	23.89 ± 0.32
PC/CEL	6.35 ± 0.12	58.29 ± 5.06	21.05 ± 0.91
PC/GF/AgNPs	6.13 ± 0.13	55.97 ± 2.13	21.56 ± 0.21
PC/CF/AgNPs	6.25 ± 0.12	58.59 ± 4.38	15.02 ± 0.39
PC/BF/AgNPs	6.18 ± 0.16	57.44 ± 7.55	20.56 ± 0.72
PC/CEL/AgNPs	6.09 ± 0.11	52.86 ± 4.90	14.36 ± 0.11

As shown in TABLES 2 and 3, the impact strength of pure HDPE equalled 7.18 kJ/m², and pure PC 6.71 kJ/m², indicating that unmodified HDPE exhibited superior toughness. However, the addition of reinforcements (BF, CF, GF, CEL) and AgNPs decreased the impact strength in both matrices. This aligns with the trends reported by Thomason, J. L. [21].

Among the tested composites, PC/CEL/AgNPs and HDPE/CEL/AgNPs demonstrated the lowest impact strength, at 6.09 kJ/m² and 5.45 kJ/m², respectively. This suggests that the combination of cellulose and silver nanoparticles reduces the material's ability to absorb energy during impact. The reduced impact strength can be attributed to the rigidity of cellulose and silver nanoparticles, which act as stress concentration sites. These sites promote crack initiation and propagation, making the composite material more brittle.

Among the reinforced PC composites, impact strength values ranged between 6.35 and 6.53 kJ/m², with AgNPs slightly reducing the overall performance. Additionally, CF had a more significant influence on the impact strength of its composites compared to GF, corroborating findings in [22].

Elongation at break measurements revealed that pure HDPE had the highest ductility, with an elongation of 375.31 ± 42%, allowing significant stretching before failure. However, adding reinforcements resulted in a reduction of ductility, with the addition of AgNPs further decreasing it. HDPE/CEL/AgNPs exhibited the lowest elongation at break at 262.51%. PC composites displayed significantly lower elongation at break (14.36%–28.51%) compared to HDPE. The lowest value was observed for PC/CEL/AgNPs at 14.36%, emphasising the negative impact of this combination on ductility. Among the HDPE and PC composites, CF caused a greater reduction in ductility than GF, consistent with findings in [22].

Composites reinforced with CF showed the highest tensile strength in both HDPE and PC groups. Notably, PC/CF displayed a tensile strength of 63.42 MPa, significantly higher than HDPE/CF at 27.99 MPa. These results align with prior studies demonstrating that CF-reinforced polymers exhibit greater tensile strength than those reinforced with BF. BF-reinforced composites consistently outperformed GF-reinforced ones in tensile strength across both matrices, as can also be observed in other studies [22-24]. Among reinforced composites, CEL exhibited the lowest tensile strength, indicating its limited contribution to load-bearing capacity. The inclusion of AgNPs reduced the tensile strength of fibre-reinforced composites. The tensile strength hierarchy for reinforcements was CF > BF > GF > CEL, with or without incorporation of AgNPs.

The tensile strength of the composites improved with the addition of fibre reinforcements. This enhancement can be attributed to the high stiffness and load-bearing capacity of the fibres that were used as reinforcements, which increased the composites' overall rigidity. However, as tensile strength improved, the composites became more brittle, leading to a reduction in impact strength. Tensile strength values varied among the samples, with HDPE composites generally exhibiting lower tensile strength than PC [25].

The antimicrobial activity of the composites was assessed to evaluate the efficacy of AgNPs in inhibiting bacterial growth. TABLE 4 presents the antibacterial performance of each material, where R represents the difference in the logarithmic number of viable bacteria between treated and untreated surfaces. For interpretive clarity, the results are grouped by R value ranges to clearly indicate the level of antibacterial effectiveness. The classification thresholds were defined as follows: Low for $R < 1.0$ (less than 90% bacterial reduction), Moderate for $1.0 \leq R < 2.0$ (90–99% reduction), High for $2.0 \leq R < 3.0$ (99–99.9% reduction), and Very High for $R \geq 3.0$ (≥99.9% reduction).

As expected, unmodified HDPE and PC samples exhibited no inherent antimicrobial activity. Similarly, the addition of fibres alone, particularly cellulose, did not result in a significant antibacterial effect. Moderate antimicrobial activity was observed in composites reinforced with carbon fibre, basalt fibre, and glass fibre, even in the absence of AgNPs. This may be attributed to minor surface effects or physical properties that slightly inhibited bacterial adhesion and proliferation.

A notable increase in antimicrobial activity was achieved through the incorporation of AgNPs. Composites containing both AgNPs and either CF or GF showed consistently high or very high antibacterial activity, with R values frequently exceeding 3.0, corresponding to ≥99.9% bacterial reduction. In particular, the PC/GF/AgNPs and HDPE/GF/AgNPs composites exhibited the highest activity levels, followed closely by their CF-reinforced counterparts. In contrast, CEL/AgNPs composites demonstrated only moderate antimicrobial efficacy, regardless of the polymer matrix used. This reduction in performance is likely due to the intrinsic properties of cellulose fibres, which may interfere with AgNP dispersion or surface exposure. Basalt fibre composites exhibited an intermediate response. HDPE/BF/AgNPs and PC/BF/AgNPs achieved “High” antimicrobial classifications, although their performance was still inferior to that of GF- and CF-reinforced systems. These results suggest that the antimicrobial behaviour of the composites is not solely determined by the presence of AgNPs but is also strongly modulated by the type of fibre reinforcement.

The observed variation in antimicrobial efficacy among composites reinforced with different fibres may be attributed to a combination of surface chemistry, nanoparticle distribution, and composite morphology. Glass and carbon fibres, due to their chemically inert and hydrophobic nature, likely support a more uniform dispersion of AgNPs across the surface. This minimizes agglomeration and maximizes nanoparticle exposure, enhancing antibacterial effectiveness. In contrast, the hydrophilic and porous structure of cellulose fibres may promote silver nanoparticle entrapment or uneven distribution, thereby reducing their accessibility for microbial inhibition. These findings collectively underscore the importance of substrate selection in designing fibre-reinforced composites with antibacterial functionality. While AgNPs are clearly effective antibacterial agents, their performance is strongly influenced by how they interact with and distribute across the fibre-matrix system.

TABLE 4. Antimicrobial activity of the composites

Composite Type	Antimicrobial Activity
PC	Low (No inherent antimicrobial properties)
PC/CEL	Low (Cellulose reinforcement does not enhance antimicrobial effects)
PC/CF	Moderate (Carbon fibres provide limited antimicrobial resistance)
PC/BF	Moderate (Basalt fibres contribute slightly, but without AgNPs, activity is not significant)
PC/GF	Moderate to High (Glass fibres have some antimicrobial benefits)
PC/CEL/AgNPs	Moderate (Silver enhances antimicrobial activity, but cellulose reduces AgNP efficiency)
PC/BF/AgNPs	High (Basalt and AgNPs contribute to significant bacterial inhibition)
PC/CF/AgNPs	High (Carbon fibres combined with AgNPs improve antimicrobial effects)
PC/GF/AgNPs	Very High (Best performance – glass fibres and AgNPs enhance bacterial reduction)
HDPE	Low (No antimicrobial properties)
HDPE/CEL	Low (Similar to PC, cellulose does not contribute significantly)
HDPE/CF	Moderate (Carbon fibre reinforcement provides some resistance)
HDPE/BF	Moderate (Basalt fibre shows slight antimicrobial effects)
HDPE/GF	Moderate to High (Glass fibre contributes to bacterial reduction)
HDPE/CEL/AgNPs	Moderate (AgNPs provide some antimicrobial properties, but cellulose reduces effectiveness)
HDPE/BF/AgNPs	High (Combination of basalt and AgNPs improves inhibition)
HDPE/CF/AgNPs	High (Carbon fibres and AgNPs enhance antimicrobial properties)
HDPE/GF/AgNPs	Very High (Best performance – glass fibres and AgNPs maximise antibacterial effect)

Conclusion

The introduction of AgNPs generally resulted in a decrease in impact strength, elongation at break, and tensile strength for both HDPE and PC composites. This indicates that while AgNPs enhance certain properties, such as antimicrobial activity, they may compromise mechanical integrity in composites made with other reinforcements. Comparing the composites made from the two matrix materials, HDPE-reinforced composites show better ductility but have lower stiffness and strength compared to PC-reinforced composites. Due to the good dispersion of reinforcements in the modified composites, a 1 wt.% reinforcement is enough to cause significant changes in the mechanical properties of matrix materials in terms of elasticity, impact strength and ductility. The composites reinforced with AgNPs exhibited significant antimicrobial activity against both Gram-negative and Gram-positive bacteria, with AgNPs in combination with GF and CF demonstrating the most pronounced effects. The observed reductions in mechanical properties of composites with double reinforcements suggest the need for optimisation in the material composition, potentially through adjusting the fibre reinforcement and AgNPs ratios or modifying processing conditions to improve the compatibility and dispersion of AgNPs.

Acknowledgements

The work was carried out as part of the statutory research of the Institute of Biomedical Engineering, University of Silesia, Katowice.

References

[1] Khan M.A., Riaz S., Ali I., Akhtar M.N., Murtaza G., Ahmad M., Shakir I., Warsi M.F.: Structural and magnetic behavior evaluation of Mg–Tb ferrite/polypyrrole nanocomposites. Ceram. Int. 41 (1, Part A) (2015) 651–656.
[2] Li X., Si H., Niu J.Z, Shen H., Zhou C., Yuan H., Wang H., Ma L., Li L.S.: Size-controlled syntheses and hydrophilic surface modification of Fe3O4, Ag, and Fe3O4/Ag heterodimer nanocrystals, Dalton Trans. 39 (45) (2010) 10984–10989.
[3] Palza H.: Antimicrobial polymers with metal nanoparticles. Int. J. Mol. Sci. 16 (2015) 2099–2116.
[4] Nasar G., Khan M.S., Khalil U.: A study on structural, mechanical and thermal properties of polymer composites of poly(vinyl alcohol) with inorganic material. Macromol. Symp. 298 (1) (2010) 124–129.
[5] Zhang R., Lin W., Moon K., Wong C. P.: Fast Preparation of printable highly conductive polymer nanocomposites by thermal decomposition of silver carboxylate and sintering of silver nanoparticles, ACS Appl. Mater. Interfaces 2 (9) (2010) 2637–2645.
[6] Li W.-R., Xie X.B., Shi Q.S., Zeng H.Y.: Antibacterial activity and mechanism of silver nanoparticles on Escherichia coli. Appl. Microbiol. Biotechnol. 85 (2010) 1115–1122.
[7] Tran Q.H., Van Nguyen Q., Le A.: Silver nanoparticles. Adv. Natl. Sci. Nanosci. Nanotechnol. 4 (2013) 33001–33021.
[8] Abdelwahab N.A., Shukry N.: Synthesis, characterization and antimicrobial properties of grafted sugarcane bagasse/silver nanocomposites. Carbohydr. Polym. 115 (2015) 276–284.
[9] Fiore V., Scalici T., Di Bella G., Valenza A.: A review on basalt fibre and its composites. Composites Part B: Engineering, 74 (2015) 74–94
[10] Chowdhury I.R., Pemberton R., Summerscales J.: Developments and Industrial Applications of Basalt Fibre Reinforced Composite Materials. J. Compos. Sci. 6 (2022) 367.
[11] Lopresto V., Leone C., De Iorio I.: Mechanical characterisation of basalt fibre reinforced plastic. Composites Part B: Engineering 42(4) (2011) 717–723.
[12] Wu D., Jing L., Peng S., Jing W.A.: Study on the Mechanical Properties of Glass-Fiber-Reinforced Defective Gypsum Boards. Sustainability 16 (2024) 821.
[13] Morampudi P., Namala K.K., Gajjela Y.K., Barath M., Prudhvi G.: Review on glass fiber reinforced polymer composites. Materials Today: Proceedings 43 (2020) 314–319.
[14] Stickel J.M., Nagarajan M.: Glass Fiber-Reinforced Composites: From Formulation to Application. International Journal of Applied Glass Science 3(2) (2012) 122–136.
[15] Abdul Khalil, H.P.S., Bhat A.H., Yusra A.F.: Green composites from sustainable cellulose nanofibrils: A review. Carbohydrate Polymers 87(2) (2012) 963–979.
[16] El Bourakadi K., Semlali F., Hammi M., El Achaby M.: A review on natural cellulose fiber applications: Empowering industry with sustainable solutions. International Journal of Biological Macromolecules 281 (2024) 135773.
[17] Seddiqi H., Oliaei E., Honarkar H., Jin J., Geonzon L.C., Bacabac R.G., Klein-Nulend J.: Cellulose and its derivatives: towards biomedical applications. Cellulose 28 (2021) 1893–1931.
[18] Chawla K.K: Composite Materials: Science and Engineering (2012, 3rd ed.). Springer Science & Business Media.
[19] Ozkan D., Gok M.S., Karaoglanli A.C.: Carbon Fiber Reinforced Polymer (CFRP) Composite Materials, Their Characteristic Properties, Industrial Application Areas and Their Machinability. In: Öchsner A., Altenbach H. (eds) Engineering Design Applications III. Advanced Structured Materials 124 (2020), Springer, Cham.
[20] Alshammari B. A., Alsuhybani M.S., Almushaikeh A.M., Alotaibi B.M., Alenad A.M., Alqahtani N.B., Alharbi A.G.: Comprehensive Review of the Properties and Modifications of Carbon Fiber-Reinforced Thermoplastic Composites. Polymers 13(15) (2020) 2474.
[21] Thomason J.L.: The influence of fibre length and concentration on the properties of glass fibre reinforced polypropylene: Part 3. Strength and strain at failure. Composites Part A: Applied Science and Manufacturing 37(11) (1996) 1922–1938.
[22] Elanchezhian C., Vijaya Ramnath B., Hemalatha J.: Mechanical Behaviour of Glass and Carbon Fibre Reinforced Composites at Varying Strain Rates and Temperatures. Procedia Materials Science 6 (2014) 1405–1418.
[23] Fiore V., Di Bella G., Valenza A.: Glass-basalt/epoxy hybrid composites for marine applications. Mat. Des. 32 (2011) 2091–2099.
[24] Liu X.H.J.: Comparison and characteristics of continuous basalt fiber, carbon fiber, aramid fiber and glass fiber. Shanxi Science and Technology 29 (2014) 87–90.
[25] Hafad S.A., Hamood A.F., AlSalihi H.A., Ibrahim S.I., Abdullah A.A., Radhi A.A., Al-Ghezi M.K., Alogaidi B.R.: Mechanical properties study of polycarbonate and other thermoplastic polymers. Journal of Physics: Conference Series 1973 (2021) 012130.